Tracking energy transfer between light harvesting complex 2 and 1 in photosynthetic membranes grown under high and low illumination

Larry Lüer[a,1], Vladimíra Moulisová[b], Sarah Henry[c], Dario Polli[d,e], Tatas H. P. Brotosudarmo[c,f], Sajjad Hoseinkhani[d,g], Daniele Brida[d], Guglielmo Lanzani[d,e], Giulio Cerullo[d], and Richard J. Cogdell[c]

[a]Madrid Institute for Advanced Studies, Department of Nanoscience, 28049 Cantoblanco, Spain; [b]Faculty of Medicine, University of Glasgow, Glasgow G12 8QQ, United Kingdom; [c]Institute for Molecular Biology, University of Glasgow, Glasgow G12 8TA, United Kingdom; [d]National Research Council, Institute of Photonics and Nanotechnologies, Dipartimento di Fisica, Politecnico di Milano, 20133 Milan, Italy; [e]Italian Institute of Technology, Center for NanoScience and Technology at Milan Polytechnic University, 20133 Milan, Italy; [f]Ma Chung Research Center for Photosynthetic Pigments, Ma Chung University, Malang 65151, Indonesia; [g]Department of Material Science, Università di Milano Bicocca, 20125 Milan, Italy

Edited by Robin M. Hochstrasser, University of Pennsylvania, Philadelphia, PA, and approved November 11, 2011 (received for review August 18, 2011)

Energy transfer (ET) between B850 and B875 molecules in light harvesting complexes LH2 and LH1/RC (reaction center) complexes has been investigated in membranes of *Rhodopseudomonas palustris* grown under high- and low-light conditions. In these bacteria, illumination intensity during growth strongly affects the type of LH2 complexes synthesized, their optical spectra, and their amount of energetic disorder. We used a specially built femtosecond spectrometer, combining tunable narrowband pump with broadband white-light probe pulses, together with an analytical method based on derivative spectroscopy for disentangling the congested transient absorption spectra of LH1 and LH2 complexes. This procedure allows real-time tracking of the forward (LH2 → LH1) and backward (LH2 ← LH1) ET processes and unambiguous determination of the corresponding rate constants. In low-light grown samples, we measured lower ET rates in both directions with respect to high-light ones, which is explained by reduced spectral overlap between B850 and B875 due to partial redistribution of oscillator strength into a higher energetic exciton transition. We find that the low-light adaptation in *R. palustris* leads to a reduced elementary backward ET rate, in accordance with the low probability of two simultaneous excitations reaching the same LH1/RC complex under weak illumination. Our study suggests that backward ET is not just an inevitable consequence of vectorial ET with small energetic offsets, but is in fact actively managed by photosynthetic bacteria.

bacteriochlorophylls | ultrafast spectroscopy

Purple bacteria are anaerobic photosynthetic prokaryotes that constitute excellent model systems for investigating the basic mechanisms of photosynthetic light harvesting (1). On the one hand, there is a very large amount of structural information from X-ray crystallography, with resolution down to the atomic scale (2–4); on the other hand, unlike in plants, there is a very clear separation between the absorption spectra of the different pigment groups (5, 6), making it easy to study the cascade of energy transfer (ET) processes funneling the excitation to the photosynthetic reaction center (RC). The photosynthetic unit (PSU) of purple bacteria, such as *Rhodopseudomonas acidophila*, is made up of two light-harvesting (LH) pigment–protein complexes, called the LH2 and the LH1/RC core complex (see Fig. 1*A*). Both these complexes are constructed from similar building blocks, consisting of oligomers of low molecular weight, hydrophobic apoproteins (called α and β), which noncovalently bind a small number of bacteriochlorophylls (BChl a, in the following referred to as BChl) and carotenoids. In the LH2 complexes, there are both monomeric BChls, with the Q_y transition at 800 nm (B800), and a ring of tightly coupled BChls, which form an excitonic band absorbing at 850 nm (B850). The LH1/RC complex only has the tightly coupled BChls, with excitonic transition at 875 nm (B875). The energetic offsets of the respective exciton resonances ensure efficient vectorial forward ET from LH2 to LH1, and from the LH1 toward the RC (7). However, because the offset between B850 and B875 is only around 40 meV, backward ET from LH1 to LH2 is also possible. Both forward and backward ET processes are indicated in Fig. 1*A* with respective rates k_F and k_B.

In the PSU, LH2 complexes surround the LH1/RC complexes in a two-dimensional network, the size and composition of which is controlled by a range of environmental conditions, including oxygen tension, incident light intensity, and light quality (8–10). In the case of the most studied purple photosynthetic bacterium *Rhodobacter sphaeroides*, the LH complexes and RCs are only synthesized when the oxygen tension is below a critical value (11, 12). Then if cells are grown at high light intensities, the PSU is dominated by LH1/RC core complexes (13, 14). If the light intensity is reduced, the size of the PSU is increased by the addition of LH2 complexes (8). A comparison of cells grown at high light (HL) and low light (LL) intensities reveals that both the number of PSUs per cell and their size increase as the incident light intensity is reduced (8, 15). This adaptation to lower light intensities clearly enhances the cells' ability to absorb incident photons in an attempt to minimize the effect of decreasing light intensity on growth.

Other species, such as *R. acidophila* and *Rhodopseudomonas palustris*, containing a multigene family of genes encoding the α- and β-apoproteins of the LH2 complexes (16, 17), show an additional response to LL intensities. In both these species, the light intensity also controls which members of the LH2 multigene family are expressed, so that different spectroscopic forms of LH2 are synthesized at LL and HL, with different apoprotein compositions (18, 19). In LL, *R. acidophila* develops a 800–820 complex toward which there is less backward ET, allowing the species to better sustain their growth under reduced illumination (20). In *R. palustris* the HL form of LH2 has its major near-infrared absorption band at 850 nm, whereas in the LL form, this band has a strongly reduced intensity and is slightly blue shifted (21). Previous studies have suggested that the lower cross-section of absorbance at 850 nm might result in reduced backward ET from LH1 and that this could allow for an increased probability

Author contributions: G.L., G.C., and R.J.C. designed research; L.L., V.M., S. Henry, D.P., T.H.P.B., S. Hoseinkhani, and D.B. performed research; L.L. contributed new reagents/analytic tools; L.L. analyzed data; and L.L., V.M., D.P., T.H.P.B., G.C., and R.J.C. wrote the paper.

The authors declare no conflict of interest.

This article is a PNAS Direct Submission.

[1]To whom correspondence should be addressed. E-mail: larry.luer@imdea.org.

This article contains supporting information online at www.pnas.org/lookup/suppl/doi:10.1073/pnas.1113080109/-/DCSupplemental.

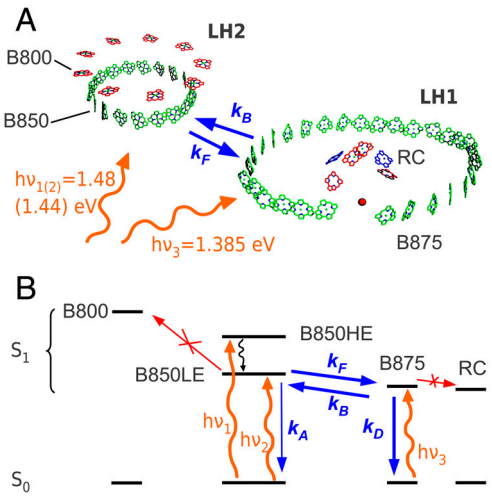

Fig. 1. (*A*) Schematic of the BChls in LH2 and LH1/RC complexes from *R. palustris*. Straight and wiggly arrows represent the forward/backward ET processes and the pump photon energies, respectively. (*B*) Energy level scheme of the processes involved in the experiment. Orange wiggly arrows, pump pulses; blue straight arrows, excitonic population transfer processes considered in the kinetic modeling; black wiggly line, ultrafast exciton relaxation; red arrows, processes that can be disregarded under the conditions of the experiment.

of successful trapping of the excitation by the RC at low illumination (22, 23).

In the present study, we address the fundamental problem of understanding what selective advantage the acquisition of the LL LH2 complex might give to *R. palustris*. To answer this question, we set out to track the real-time evolution of the relative excited state population densities in LH2 and LH1 following selective photoexcitation. We use a specially designed femtosecond pump-probe spectrometer, combining tunable narrowband pump with broadband white-light probe pulses, and introduce an analytical method based on derivative spectroscopy for disentangling the congested transient absorption spectra of LH1 and LH2 complexes. In previous femtosecond studies (24, 25), the contributions of forward and backward ET to the observed LH2 ↔ LH1 equilibration dynamics could not be resolved, and therefore information on backward ET has only been obtained in an indirect and qualitative manner (20, 26, 27). With our approach, we are able to track the equilibration dynamics, determine both forward and backward ET rate constants, and quantify the final population equilibrium between B850 and B875 excitons (see Fig. 1). We observe that LL samples have lower ET rates in both directions with respect to HL ones, explained by reduced spectral overlap between B850 and B875 due to partial redistribution of oscillator strength into a higher energetic exciton transition. We find that the LL adaptation in *R. palustris* leads to a reduced elementary (i.e., between individual LH complexes) backward ET rate, in accordance with the low probability of two simultaneous excitations reaching the same LH1/RC complex under weak illumination. Our study suggests that backward ET is not just an inevitable consequence of vectorial ET with small energetic offsets, but is in fact actively managed by photosynthetic bacteria to adapt to changing illumination conditions.

Results and Discussion

Ground-State Absorption Spectra. Ground-state absorption spectra of suspensions of HL(LL)-grown photosynthetic membranes from *R. palustris* are shown in Fig. 2 *A* and *B*. They are characterized by a relatively sharp absorption band at 1.55 eV and a broad absorption band from 1.35 to 1.5 eV. In agreement with previous work (23), the spectra of LH2 complexes of LL membranes were modeled by a superposition of a sharp band at

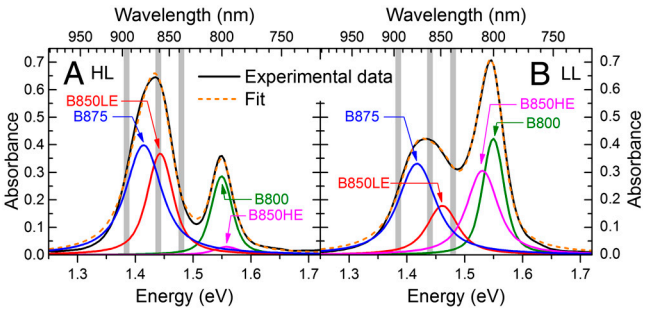

Fig. 2. Ground-state absorption spectrum (black solid line) of HL (*A*) and LL (*B*) membranes of *R. palustris*, together with fits (orange dashed line) with Voigt band shapes. The gray bands represent the three pump photon energies used.

1.55 eV, assigned to the B800 chromophores, and broader bands at 1.45 and 1.53 eV, associated to the low-energy (LE) and high-energy (HE) excitons of the B850 rings, respectively; in the HL bacteria, the HE exciton is only weakly coupled to the ground state. The B875 rings from LH1 contribute to the low-energy part of the absorption band around 1.4 eV. This spectral congestion complicates the assignment of the different bands, that we modeled by Voigt profiles. We first obtained their widths with high accuracy fitting the second derivatives of the spectra (see *Materials and Methods*). Then we fitted the spectra in Fig. 2 using as free parameters the spectral weights and the center positions, with the ratio B800/(B850LE + B850HE) fixed to 0.544, which is the value found in isolated HL-grown LH2 complexes (*SI Text*). We find that in HL(LL) samples the LH2 complexes contribute for 51%(64)% of the spectral weight, confirming the well-known fact that, under LL conditions, the ratio LH1:LH2 in *R. palustris* is significantly shifted toward LH2 (28). An increasing contribution of LH2 complexes in membranes isolated from this bacterial species grown at LL conditions has also been visualized by atomic force microscopy (15).

Transient Absorption Spectra of Membranes. The time-resolved experiments were performed on photosynthetic membranes with closed RC, because the concomitant suppression of ET from B875 to the RC increases the lifetime of the B875 exciton, facilitating the study of backward ET (for details see *SI Text*). Fig. 3 *A* and *C* show transient absorption (TA) spectra of LL membranes

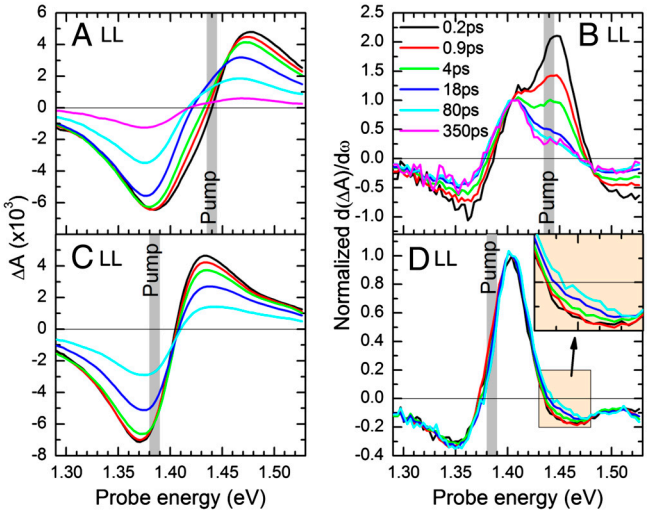

Fig. 3. (*A* and *C*) Δ*A* spectra of LL membranes pumped 1.44 and 1.385 eV at selected pump-probe delays; (*B* and *D*) corresponding first derivatives of the Δ*A* spectra, normalized at 1.405 eV. (*D*, *Inset*) A zoom into the region around 1.45 eV to highlight the monotonous increase of signal.

after pumping with pulses centered at 1.44 and 1.385 eV photon energy, predominantly resonant with the B850 of LH2 and the B875 of LH1, respectively (see also Fig. 2*B*). The differential absorption (ΔA) spectra are characterized by a negative band around 1.385 eV and a positive band of similar strength around 1.45 eV. These bands are attributed to the superposition of the photobleaching (PB) of the B875 and B850 excitons and of their photoinduced absorption (PA) due to exciton-to-biexciton transitions.

In order to assess rate constants for LH2 ↔ LH1 ET processes, we need to extract the relative population of the B850 and B875 excitons as a function of time. This extraction is complicated by the energetic congestion of the LH1 and LH2 transitions, which are only 40 meV apart. The spectral separation can be greatly enhanced by plotting the first derivatives of the ΔA spectra, $d(\Delta A)/d\omega$, as explained in detail in *Materials and Methods*. We note that, because the numerical derivative process increases the noise in the spectra, this analysis is only made possible by the very high signal-to-noise ratio of our optimized broadband pump-probe system. Fig. 3 *B* and *D* display the first derivatives of the ΔA spectra in Fig. 3 *A* and *C*, respectively, normalized to the B875 peak. We find that the first derivatives clearly show maxima at 1.41 and 1.45 eV, precisely at the peaks of the B875 and B850 excitonic transitions, whose relative weight changes with pump-probe delay.

When pumping at 1.44 eV (Fig. 3*B*), we find that the population initially resides predominantly on B850, confirming our selective pumping condition. The spectral weight then shifts to B875, indicating forward B850 → B875 ET, within a few picoseconds, a timescale comparable to similar systems (24, 25). However, even after 350 ps, a considerable amount of B850 population remains, indicating a backward B850 ← B875 ET, leading to a stationary B850/B875 ratio after an equilibration dynamics.

When pumping at 1.385 eV (Fig. 3*D*), we observe that the population resides predominantly on the B875, with very little spectral evolution over time. When zooming into the B850 region at 1.45 eV (see Fig. 3*D*, *Inset*), we find that there is a slight increase of the relative B850 population on an approximately 10 ps timescale, again indicating a backward ET. Note that an increase of the relative B850 population can alternatively be explained by a higher annihilation rate in B875 than in B850. We can exclude this scenario, because (*i*) we quantified annihilation in both HL and LL samples, and found it to influence the early dynamics of HL samples (where mainly B850 is populated), whereas it is negligible in LL samples (see *SI Text*); (*ii*) we observe a constant long-time B850/B875 population ratio. Note that the spectral shapes of Fig. 3 *B* and *D* at 80 ps (cyan curves) clearly differ from each other, meaning that, after pumping at 1.44 and 1.385 eV, equilibria are reached that differ in the ratio B850/B875. We generally observe this effect in LL samples but not in HL samples, which points to inhomogeneous broadening of the B875 exciton in the LL samples.

Forward and Backward ET Rate Constants. In Fig. 4 *A* and *C*, we show as data points the first derivatives of the ΔA spectra of HL and LL samples, respectively, pumped at 1.44 eV. The fits (solid lines), according to the multi-Voigt analysis described in *Materials and Methods*, reproduce the experimental data without systematic deviations, at all time delays. The resulting time-dependent spectral weights, which are proportional to the populations of B850 and B875 excitons, are shown as data points in Fig. 4 *B* and *D* for HL and LL samples, respectively. The availability of time-dependent populations of B850 and B875 exciton allows the direct time-domain extraction of the rates for both the forward (B850 → B875) and backward (B850 ← B875) ET processes (k_F and k_B, respectively; see Fig. 1*A*). We use the following kinetic model for the excitonic populations (see Fig. 1*B*):

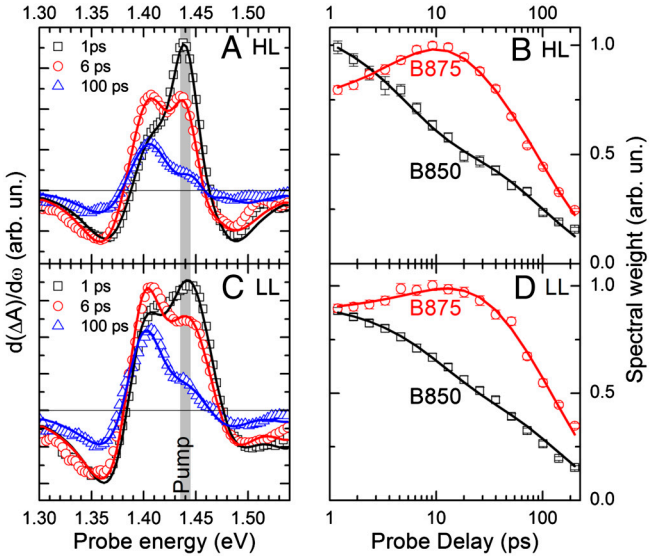

Fig. 4. (*A* and *C*) First derivatives of ΔA spectra of HL and LL samples, pumped at 1.44 eV (symbols) and fits according to the model presented in the text (solid lines). (*B* and *D*) Time-dependent B850 and B875 spectral weights (symbols) as obtained from the fits of panels *A* and *C*, and corresponding fits according to the kinetic model presented in the text (solid lines).

$$d\mathrm{B850}/dt = -k_F\mathrm{B850} + k_B\mathrm{B875} - k_A\mathrm{B850}^2, \qquad [1a]$$

$$d\mathrm{B875}/dt = k_F\mathrm{B850} - k_B\mathrm{B875} - k_D\mathrm{B875}, \qquad [1b]$$

where k_D is the B875 deactivation rate and k_A accounts for B850 deactivation by bimolecular exciton annihilation (see *SI Text*). The resulting fits are shown in Fig. 4 *B* and *D* as solid lines, and the corresponding rates are summarized in Table 1. We can draw the following conclusions: (*i*) for both HL and LL samples, the ratio k_F/k_B is close to two; (*ii*) for LL samples, both k_F and k_B are a factor of two smaller than in HL samples; (*iii*) in both samples, k_F and k_B do not depend on the pump photon energy.

Discussion

Our results can be put in the context of previous ultrafast spectroscopy studies, which have probed the dynamics of both intra- and intercomplex ET processes within the PSU (29–32). It was found that B800 → B850 ET in the LH2 proceeds with a time constant of approximately 1 ps, with virtually no backward ET (33). Exciton hopping between B850 rings of different LH2 complexes occurs with an approximately 10 ps time constant. The LH2 ↔ LH1 ET dynamics, which is the focus of the present paper, has been studied comparatively little. Although LH2 → LH1 forward ET has been studied in membranes of *R. sphaeroides* (24, 25), none of these studies observed the LH2 ← LH1 backward ET in the time domain, even following selective pumping of the B875. Backward ET has been studied only by indirect methods, such as the change in photoluminescence from B850 upon chemically modifying B875 (20, 26, 27). Although these studies

Table 1. Forward ET (k_F), backward ET (k_B), and B875 (k_D) deactivation rates for the different samples and pumping conditions

Sample/pump photon energy, eV	$1/k_F$, ps	$1/k_B$, ps	$1/k_D$, ps
HL/1.44	9 (1)	16 (2)	120 (5)
HL/1.48	10 (2)	20 (5)	84 (3)
LL/1.44	17 (2)	36 (5)	134 (5)
LL/1.48	19 (3)	38 (9)	141 (10)

Values in brackets are errors.

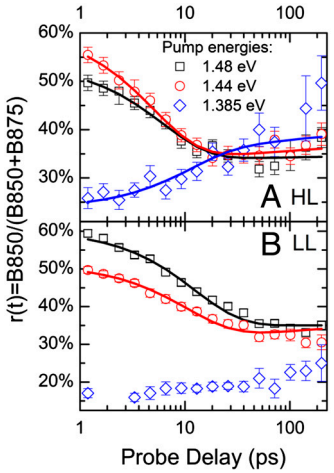

Fig. 5. Time-dependent relative B850 population $r(t) = \mathrm{B850}(\mathrm{B850} + \mathrm{B875})$ for HL (*A*) and LL (*B*) samples and different pumping conditions (symbols) and fits according to the model described in the text (solid lines).

clearly showed backward ET to occur, they did not provide the respective rate constants and the equilibration dynamics.

The LH2 ↔ LH1 ET rates have been derived theoretically on the basis of the atomic-level structures of the pigment–protein complexes in *Rhodospirillum molischianum* and of an effective Hamiltonian for intracomplex excitations (34). A forward LH2 → LH1 ET rate $k_F = 1/7.7$ ps^{-1} and a backward LH2 ← LH1 ET rate $k_B = 1/15.5$ ps^{-1} were calculated, in remarkably good agreement with our experimental data for the HL membranes (see Table 1).

To get a deeper insight in the LH2 ↔ LH1 equilibration dynamics, it is instructive to plot (see Fig. 5) the *relative* B850 population $r(t) = \mathrm{B850}(t)/[\mathrm{B850}(t) + \mathrm{B875}(t)]$, which directly shows the interplay between forward and backward ET leading to the establishment of an equilibration. In the hypothesis k_F, $k_B \gg k_D$, and $k_A \approx 0$, which is reasonably well satisfied in our case, Eq. **1** can be analytically solved to give

$$r(t) = r_\infty + (r_0 - r_\infty)\exp[-(k_F + k_B)t], \qquad [2]$$

where $r_0 = r(0)$ is the initial value, and $r_\infty = k_B/(k_F + k_B)$ is the equilibrium value, which can be higher or lower than r_0 according to the pumping conditions. In this approximation, the rate for the equilibration process is the sum of the forward and backward ET rates. Fig. 5 indicates that an equilibration between B850 and B875 is indeed established at long times. The presence of this equilibrium shows the absence of any significant amount of isolated LH2 complexes without ET pathways toward LH1. Excitons on such isolated LH2 complexes could only decay with the intrinsic lifetime of B850 excitons, which is much longer than that of B875 (23), and therefore $r(t)$ would continuously increase rather than becoming constant.

Fig. 5 shows that r_0 depends strongly on the pump photon energy. We were able to vary r_0 from below 0.2 (pumping at 1.385 eV, predominantly exciting B875) to about 0.6 (pumping at 1.48 eV, predominantly exciting B850). All relative B850 populations reach a constant final ratio r_∞ of approximately 0.35 after tens of picoseconds, irrespective of the pump photon energy, except for the LL sample pumped at 1.385 eV (see below). This value for r_∞ means that any given exciton dwells for about 65% of its lifetime on the LH1 complex where the photosynthetic RC is located, ready to accept the energy after being reduced again, and where charge separation can take place.

Note that the values for k_F and k_B, as obtained from Eq. **2**, are ensemble rate constants, which are related to the elementary rate constants by considering the probability of transfer events, which depends on the relative abundance LH2 : LH1. Considering the fact that, in LL samples, the ratio LH2 : LH1 is much higher than in HL samples (about 1:1 and 2:1 for HL and LL, respectively, as obtained from the respective spectral weights in Fig. 2), one would expect the corresponding r_∞ to be higher because the LH1 is surrounded by more LH2s, which could receive the back-transferred excitation. The fact that we observe, within the experimental error, the same r_∞ in HL and LL samples, means that the ratio of the elementary rate constants in LL membranes is clearly shifted toward forward ET, strongly reducing backward ET. This effect can be explained straightforwardly by reduced spectral overlap between B850 and B875 in LL compared to HL samples, caused by a "splitting" (partial redistribution of oscillator strength) of the B850 exciton resonance into two bands at 1.45 (B850LE) and 1.53 eV (B850HE), respectively (23), having similar spectral weights. Note that the presence of backward ET in HL samples is a clear advantage for efficient photosynthesis because it avoids exciton trapping on B875 sites with momentarily oxidized RC (because of a charge transfer event that occurred a short time before the second exciton arrived). The exciton has thus the opportunity to "try" a different LH1 complex. Because this scenario is much less probable under LL conditions, backward ET is less important in LL samples. Finally, by direct comparison of the solid lines in Fig. 5 *A* and *B*, we note that, in the LL-grown bacteria, the equilibration dynamics is about two times slower than for the HL samples, because both the k_F and k_B rates are reduced.

The final relative B850 population r_∞ reached for the LL sample pumped at 1.385 eV is clearly lower than the values reached for the other pump photon energies and for the HL grown bacteria. This effect is also clearly visible in Fig. 3*D*, where (see inset) upon pumping at 1.385 eV, the signal in the 1.45 eV region normalized to the signal at 1.405 eV (thus indicating the B850 population relative to the B875 one) at long time delays is much weaker than that in Fig. 3*B*, relative to the same LL sample with excitation at 1.44 eV. This observation can be explained by the presence in the LL membranes of a higher disorder (23) and a lower B850 → B850 ET rate in comparison to HL membranes, as confirmed by exciton annihilation measurements (see *SI Text*). As indicated by the left gray-shaded area in Fig. 2*B*, the 1.385 eV pump photon energy is located in the red edge of the B875 band: In the presence of disorder, a subset of red-shifted excitons will be excited, thus reducing the backward ET due to the increased energy gap. This increased energy gap leads to an equilibrium strongly on the side of the B875, in agreement with the lower r_∞ value that we find. In contrast, when pumping resonantly the B850 excitons, the equilibrium will take place with the most abundant B875 moieties, for which r_∞ is about 0.35. In HL samples, $r_\infty = 0.35$ is reached in all experiments, even for excitons that have been created on a low-energetic B875 moiety (blue diamonds in Fig. 5*A*). The independence of r_∞ in HL membranes on the pumping conditions cannot be attributed to a reduced disorder (23). It can be most probably assigned to excitation memory loss accomplished by exciton migration from one LH1 to the other, mediated by B850 ← B875 backward ET and multiple hopping steps between B850s on adjacent LH2s. This process is considerably reduced in LL membranes, as demonstrated by the strong dependence of r_∞ on the pump energy. The excitation memory is thus conserved during the full exciton lifetime in LL membranes. This striking difference between HL and LL membranes can be rationalized by a lower rate of B850 ↔ B850 transfer (demonstrated by reduced exciton annihilation in LL samples, see *SI Text*) and by a higher average distance between LH1 complexes, due to the high abundance of LH2 complexes in LL membranes. We therefore can conclude that an exciton created on an LL membrane typically "sees" only one LH1/RC complex in its lifetime. This conclusion agrees with the above notion that, under LL conditions, a transfer to a different LH1/RC complex is rarely

necessary, because the probability that a certain RC is still oxidized, is very low.

In conclusion, we have presented a time-domain study of LH2 ↔ LH1 forward/backward ET processes in membranes of the purple bacterium *R. palustris*. Broadband femtosecond TA spectroscopy with tunable narrowband pump pulses, in combination with an analysis method based on the derivatives of the TA spectra, gave access to time-resolved populations of B850 and B875 excitons. We demonstrated that the initial populations of B850 and B875 excitons, resonantly excited by the pump pulse, undergo equilibration toward a stable relative population, within tens of picoseconds. The separate observation of both equilibration dynamics and equilibrium allows us to obtain reliable rate constants for both forward and backward ET directly in the time domain, under various experimental conditions. This analytical method can be applied to a broad range of samples; in particular, it will be interesting to characterize the light-harvesting performance of artificial photosynthetic devices obtained by assembling natural antenna complexes on surfaces with engineered architectures (35–37), in view of their optimization.

We found that LL samples of *R. palustris* have reduced ET rates in both directions, explained by reduced spectral overlap due to partial redistribution of oscillator strength into the high-energy B850 band at 1.53 eV. We observe that, after reaching equilibrium, the average dwelling time of any exciton on the LH1 complex is about 65%, even in LL complexes where the average ratio LH1:LH2 is only 1:2, meaning that the elementary backward ET process is strongly reduced in LL samples relative to HL ones. Moreover, we found that backward ET in the case of LL samples does not mediate a transfer among different LH1 complexes because it is not needed due to the weak illumination.

Our study indicates that backward ET is not just an inevitable consequence of vectorial ET with small energetic offsets, but in fact is managed actively by biological systems, in dependence of illumination intensity, in order to avoid exciton trapping if necessary. This peculiar behavior of *R. palustris* poses the question: Why did purple bacteria develop strategies for low light adaptation that vary so strongly in complexity? At present there is no definitive answer to this question. However, it is reasonable to suggest that these differences reflect the selection pressures that each species experiences in its particular habitat. Interestingly, some species of purple photosynthetic bacteria only have LH1 (e.g., *Rhodospirillum rubrum*), whereas others only have a single type of LH2 (e.g., *R. sphaeroides*). Both these types of bacteria grow successfully in the wild. Nobody has yet tried to investigate their relative competitiveness in different ecological niches as a function of the complexity of their photosynthetic apparatus, however, this would be a very interesting study.

Materials and Methods

Sample Preparation. Cells of *R. palustris* strain 2.1.6 were grown anaerobically in C-succinate medium at 30 °C at 220 (10) lux for HL (LL) conditions, harvested by centrifugation, then resuspended and homogenized. The resuspended cells were broken using a French press and the membranes were purified. In this work, we show results obtained with membranes containing closed RCs. In these samples, the energy transfer from B875 toward the RC cannot occur, which leads to an increased B875 lifetime, facilitating the observation and quantification of the equilibrium population ratio B850/B875. Nevertheless, we performed all experiments also with open RC, and confirmed the conclusions obtained from the samples with closed RC. All details of the procedures are given in the *SI Text*.

Ultrafast Spectroscopy. We have designed a special TA setup, which combines a tunable narrowband pump pulse, to enable selective excitation of the different chromophores in the membranes, with a broadband probe pulse. The system starts with an amplified Ti:sapphire laser system (1 kHz, 150 fs, 500 μJ) at the fundamental wavelength (FW) of 780 nm. The near-IR portion ($\lambda > 800$ nm, selected by a long-pass filter) of a white-light continuum (WLC), generated in a 1-mm-thick sapphire plate, is used as the probe pulse. An optical parametric amplifier (OPA), generating narrowband (*ca.* 10 meV FWHM) pulses, tunable from 820 nm (1.51 eV) to 1,050 nm (1.18 eV), is used to pump the membranes. The OPA is pumped by the second harmonic (SH) of the Ti:sapphire, generated in a 3-mm-thick ß-barium-borate (BBO) crystal. The limited acceptance bandwidth of the thick BBO crystal ensures a narrow bandwidth of the pump pulses. The seed pulses, obtained by WLC generation in a 2-mm-thick sapphire plate, are chirped by a 1-cm-thick ZnSe plate, which introduces a group delay of approximately 3 ps between the 800 and 1,050-nm wavelengths, ensuring that only a nearly monochromatic portion of the broadband seed is temporally overlapped with the pump. Pump and seed are superimposed in a 2-mm-thick BBO crystal. The narrow linewidth of the SH pump pulse ensures the generation of approximately 10-meV bandwidth pulses, with 500-nJ energy, tunable in the 1.25- to 1.5-eV range by changing the delay between pump and seed.

Pump and probe pulses, synchronized by a delay line, are focused on the sample in a noncollinear geometry, and the transmitted probe is dispersed in a spectrometer with single-shot detection capability at the full 1-kHz laser repetition rate (38) providing a sensitivity of ΔA at approximately 10^{-5}. Both these characteristics are essential for our data analysis method (see below). In order to minimize exciton–exciton annihilation, while still maintaining a signal-to-noise level sufficient for processing the TA spectra, we limited the pump pulse fluence to below 6 μJ/cm^2 (20). The overall time resolution of the setup is about 200 fs.

Data Analysis. The spectral decomposition of TA spectra of photosynthetic membranes is complicated by strong spectral overlap of a multitude of PB and PA features. Here, we circumvent these difficulties by extending derivative spectroscopy, a well-known concept in continuous wave spectroscopy of multicomponent systems (39), to time-resolved studies. The full procedure and justification is given in the *SI Text*. In short, derivative spectroscopy exploits the fact that a second derivative of any symmetric bell-shaped function (Gaussian, Lorentzian, etc.) peaks at the same spectral position as the original function, but with significantly reduced bandwidth, strongly enhancing spectral separation. Because in large aggregates the energetic offset between the excitonic PA and PB bands is much lower than the width of both bands (40), their TA spectrum can be very well approximated by the first derivative of the ground-state absorption spectrum, $\Delta A \cong A(\omega - \omega_0 - \Delta\omega) - A(\omega - \omega_0) \cong -dA/d\omega \cdot \Delta\omega$. In the *SI Text*, we show that this is the case for isolated LH2 complexes. Consequently, first derivatives of the TA spectra are to the first approximation equivalent to second derivatives of the ground-state absorption spectra, $d(\Delta A)/d\omega \cong -d^2A/d\omega^2 \cdot \Delta\omega$. The concomitant increased spectral resolution allows for direct observation of the populations of the B850 and B875 moieties and of their forward and backward ET dynamics. For this reason, we used $d(\Delta A)/d\omega$ spectra, rather that the ΔA spectra, for kinetic modeling (see *SI Text*).

ACKNOWLEDGMENTS. The authors are indebted to Cristian Manzoni for help with the experimental setup. R.J.C. acknowledges support from the Biotechnology and Biological Sciences Research Council; V.M., T.H.P.B., and S. Hoseinkhani by the European Commission (Contract MCRTN-CT- 2006-035859-BIMORE); L.L. through a Ramon y Cajal fellowship (Spanish Ministry of Science and Innovation); D.P. and R.J.C. by the Human Frontier Science Program Grant RGP0005; and DP by the "5 per mille junior" research grant by Politecnico di Milano.

1. Cogdell RJ, Gall A, Köhler J (2006) The architecture and function of the light-harvesting apparatus of purple bacteria: From single molecule to in vivo membranes. *Q Rev Biophys* 39(3):227–324.
2. McDermott G, et al. (1995) Crystal structure of an integral membrane light-harvesting complex from photosynthetic bacteria. *Nature* 374:517–521.
3. Koepke J, Hu XC, Muenke C, Schulten K, Michel H (1996) The crystal structure of the light-harvesting complex II (B800–850) from *Rhodospirillum molischianum*. *Structure* 4:581–597.
4. Roszak AW, et al. (2003) Crystal structure of the RC-LH1 core complex from *Rhodopseudomonas palustris*. *Science* 302:1969–1972.
5. Frank HA, Cogdell RJ (1996) Carotenoids in photosynthesis. *Photochem Photobiol* 63:257–264.
6. Freer A, et al. (1996) Pigment-pigment interactions and energy transfer in the antenna complex of the photosynthetic bacterium *Rhodopseudomonas acidophila*. *Structure* 4:449–462.
7. Sundström V, Pullerits T, van Grondelle R (1999) Photosynthetic light-harvesting: Reconciling dynamics and structure of purple bacterial LH2 reveals function of photosynthetic unit. *J Phys Chem B* 103:2327–2346.
8. Aagaard J, Sistrom WR (1972) Control of synthesis of reaction center bacteriochlorophyll in photosynthetic bacteria. *Photochem Photobiol* 15:209–225.

9. Evans K, et al. (2005) A bacteriophytochrome regulates the synthesis of LH4 complexes in *Rhodopseudomonas palustris*. *Photosynth Res* 85:169–180.
10. Gardiner AT, Cogdell RJ, Takaichi S (1993) The effect of growth conditions on the light-harvesting apparatus in *Rhodopseudomonas acidophila*. *Photosynth Res* 38:159–167.
11. Hunter CN, Ashby MK, Coomber SA (1987) Effect of oxygen on levels of mRNA coding for reaction-centre and light-harvesting polypeptides of Rhodobacter sphaeroides. *Biochem J* 247:489–492.
12. Roh JH, Smith WE, Kaplan S (2004) Effects of oxygen and light intensity on transcriptome expression in Rhodobacter sphaeroides 2.4.1: Redox active gene expression profile. *J Biol Chem* 279:9146–9155.
13. Drews G (1985) Structure and functional organization of light-harvesting complexes and photochemical reaction centers in membranes of phototrophic bacteria. *Microbiol Rev* 49:59–70.
14. Evans MB, Hawthornthwaite AM, Cogdell RJ (1990) Isolation and characterisation of the different B800–850 light harvesting complexes from low- and high-light grown cells of *Rhodopseudomonas palustris*, strain 2.1.6. *Biochim Biophys Acta Bioenerg* 1016:71–76.
15. Scheuring S, Goncalves RP, Prima V, Sturgis JN (2006) The photosynthetic apparatus of *Rhodopseudomonas palustris*: Structures and organization. *J Mol Biol* 358:83–96.
16. Brunisholz RA, Zuber H (1992) Structure, function and organization of antenna polypeptides and antenna complexes from the three families of Rhodospirillaneae. *J Photochem Photobiol B* 15:113–140.
17. Tadros MH, Waterkamp K (1989) Multiple copies of the coding regions for the light-harvesting B800-850 α and β polypeptides are present in the *Rhodopseudomonas palustris* genome. *EMBO J* 8:1303–1308.
18. Brotosudarmo THP, et al. (2009) Single-molecule spectroscopy reveals that individual low-light LH2 complexes from *Rhodopseudomonas palustris* 2.1.6. have a heterogeneous polypeptide composition. *Biophys J* 97:1491–1500.
19. Gardiner AT, Mackenzie RC, Barrett SJ, Kaiser K, Cogdell RJ (1996) The purple photosynthetic bacterium *Rhodopseudomonas acidophila* contains multiple puc peripheral antenna complex (LH2) genes: Cloning and initial characterisation of four β/α pairs. *Photosynth Res* 49:223–235.
20. Deinum G, et al. (1991) Antenna organization of *Rhodopseudomonas acidophila*: A study of the excitation migration. *Biochim Biophys Acta Bioenerg* 1060:125–131.
21. Cogdell RJ, Howard TD, Isaacs NW, McLuskey K, Gardiner AT (2002) Structural factors which control the position of the Q(y) absorption band of bacteriochlorophyll a in purple bacterial antenna complexes. *Photosynth Res* 74:135–141.
22. Law CJ, Cogdell RJ, Trissl HW (1997) Antenna organisation in the purple bacterium *Rhodopseudomonas acidophila* studied by fluorescence induction. *Photosynth Res* 52:157–165.
23. Moulisová V, et al. (2009) Low light adaptation: Energy transfer processes in different types of light harvesting complexes from *Rhodopseudomonas palustris*. *Biophys J* 97:3019–3028.
24. Hess S, et al. (1995) Temporally and spectrally resolved subpicosecond energy transfer within the peripheral antenna complex (LH2) and from LH2 to the core antenna complex in photosynthetic purple bacteria. *Proc Natl Acad Sci USA* 92:12333–12337.
25. Nagarajan V, Parson WW (1997) Excitation energy transfer between the b850 and b875 antenna complexes of rhodobacter sphaeroides. *Biochemistry* 36:2300–2306.
26. Woodbury NW, Parson WW, Gunner MR, Prince RC (1986) Radical-pair energetics and decay mechanisms in reaction centers containing anthraquinones, naphthoquinones or benzoquinones in place of ubiquinone. *Biochim Biophys Acta Bioenerg* 851:6–22.
27. Kramer H, et al. (1995) Energy migration in *Rhodobacter sphaeroides* mutants altered by mutagenesis of the peripheral LH2 complex or by removal of the core LH 1 complex. *Biochim Biophys Acta Bioenerg* 1231:89–97.
28. Firsow NN, Drews G (1977) Differentiation of the intracytoplasmic membrane of *Rhodopseudomonas palustris* induced by variations of oxygen partial pressure or light intensity. *Arch Microbiol* 115:299–306.
29. Pullerits T, Chachisvilis M, Jones MR, Hunter CN, Sundström V (1994) Exciton dynamics in the light-harvesting complexes of *Rhodobacter sphaeroides*. *Chem Phys Lett* 224:355–365.
30. Monshouwer R, Dezarate IO, Vanmourik F, Vangrondelle R (1995) Low-intensity pump-probe spectroscopy on the B800 to B850 transfer in the light harvesting 2 complex of *Rhodobacter sphaeroides*. *Chem Phys Lett* 246:341–346.
31. Polivka T, Pullerits T, Frank HA, Cogdell RJ, Sundström V (2004) Ultrafast formation of a carotenoid radical in LH2 antenna complexes of purple bacteria. *J Phys Chem B* 108:15398–15407.
32. Niedzwiedzki DM, Fuciman M, Frank HA, Blankenship RE (2011) Energy transfer in an LH4-like light harvesting complex from the aerobic purple photosynthetic bacterium Roseobacter denitrificans. *Biochim Biophys Acta Bioenerg* 1807:518–528.
33. Monshouwer R, van Grondelle R (1996) Excitations and excitons in bacterial light-harvesting complexes. *Biochim Biophys Acta Bioenerg* 1275:70–75.
34. Ritz T, Park S, Schulten K (2001) Kinetics of excitation migration and trapping in the photosynthetic unit of purple bacteria. *J Phys Chem B* 105:8259–8267.
35. Blankenship RE, et al. (2011) Comparing photosynthetic and photovoltaic efficiencies and recognizing the potential for improvement. *Science* 332:805–809.
36. Escalante M, et al. (2008) Nanometer arrays of functional light harvesting antenna complexes by nanoimprint lithography and host-guest interactions. *J Am Chem Soc* 130:8892–8893.
37. Gust D, Moore TA, Moore AL (2001) Mimicking photosynthetic solar energy transduction. *Acc Chem Res* 34(1):40–48.
38. Polli D, Lüer L, Cerullo G (2007) High-time-resolution pump-probe system with broadband detection for the study of time-domain vibrational dynamics. *Rev Sci Instrum* 78:103108.
39. Talsky G (1994) *Derivative Spectrophotometry* (VCH, Weinheim, Germany).
40. Van Burgel M, Wiersma DA, Duppen K (1995) The dynamics of one-dimensional excitons in liquids. *J Chem Phys* 102:20–33.